Available online at www.sciencedirect.com
ScienceDirect
Biochimica et Biophysica Acta 1784 (2008) 393–399
Biochimica et Biophysica Acta BBA
www.elsevier.com/locate/bbapap

Crystallographic structure and substrate-binding interactions of the molybdate-binding protein of the phytopathogen *Xanthomonas axonopodis* pv. *citri*

Andrea Balan [a,b], Carolina Santacruz-Pérez [a,b], Alexandre Moutran [a], Luís Carlos Souza Ferreira [a], Goran Neshich [c], João Alexandre Ribeiro Gonçalves Barbosa [b,*]

[a] *Departamento de Microbiologia, Instituto de Ciências Biomédicas II, Universidade de São Paulo, Cidade Universitária, São Paulo, SP, 05008-900, Brazil*
[b] *Center for Structural Molecular Biology (CeBiME), Brazilian Synchrotron Light Laboratory (LNLS), CP 6192, Campinas, SP, 13084-971, Brazil*
[c] *Laboratório de Bioinformática, EMBRAPA/CNPTIA, Campinas, SP, Brazil*

Received 27 August 2007; received in revised form 8 November 2007; accepted 13 November 2007
Available online 26 December 2007

Abstract

In *Xanthomonas axonopodis* pv. *citri* (*Xac* or *X. citri*), the *modA* gene codes for a periplasmic protein (ModA) that is capable of binding molybdate and tungstate as part of the ABC-type transporter required for the uptake of micronutrients. In this study, we report the crystallographic structure of the *Xac* ModA protein with bound molybdate. The *Xac* ModA structure is similar to orthologs with known three-dimensional structures and consists of two nearly symmetrical domains separated by a hinge region where the oxyanion-binding site lies. Phylogenetic analysis of different ModA orthologs based on sequence alignments revealed three groups of molybdate-binding proteins: bacterial phytopathogens, enterobacteria and soil bacteria. Even though the ModA orthologs are segregated into different groups, the ligand-binding hydrogen bonds are mostly conserved, except for *Archaeglobus fulgidus* ModA. A detailed discussion of hydrophobic interactions in the active site is presented and two new residues, Ala_{38} and Ser_{151}, are shown to be part of the ligand-binding pocket.

Keywords: ModA; Molybdate-binding protein; *Xanthomonas axonopodis* pv. *citri*; ABC transporters; X-ray crystal structure

1. Introduction

Molybdenum and tungsten are normally available in trace amounts in the environment and must be incorporated into the cells in an efficient way [1,2]. Many proteins bind molybdenum and tungsten and for molybdoenzymes such as nitrate reductase, formate dehydrogenase, dimethyl-sulfoxide reductase, trimethylamine-N-oxide reductase, and biotin-sulfoxide reductase, molybdenum is required as a cofactor [3,4]. These enzymes are responsible for transduction of energy, uptake of nutrients and gene regulation and can be found in the cytoplasm and associated with the cytoplasmic membrane [5–8].

The molybdate-binding protein (ModA) belongs to a distinct class of periplasmic proteins pertaining to the group of ABC (*A*TP-*B*inding *C*assette) transporters specifically involved in the uptake of nutrients including metals such as molybdenum [9]. Among the periplasmic nutrient-binding proteins, ModA shows the highest degree of both specificity and affinity in comparison with other soluble components of ATP-dependent uptake systems [10]. The enhanced affinity of ModA to tetrahedral oxyanions, such as molybdate and tungstate, with regard to other potential ligands including sulfate, phosphate and vanadate, was attributed either to the higher coordination number or the larger anion size [11], as deduced from the structural studies.

The structures of the *Escherichia coli* (*Eco* ModA), *Azotobacter vinelandii* (*Avi* ModA) and more recently, *Archaeglobus fulgidus* (*Afu* ModA) ModAs were solved and shown to share high structural similarities in spite of the low amino acid sequence identity [12–13]. The proteins show an ellipsoidal shape with two globular domains connected by a hinge region and delimiting a cleft where the anion is bound and remains

* Corresponding author. Tel.: +55 19 3512 1107; fax: +55 19 3512 1004.
E-mail address: joao@lnls.br (J.A.R.G. Barbosa).

1570-9639/$ - see front matter © 2007 Elsevier B.V. All rights reserved.
doi:10.1016/j.bbapap.2007.11.013

completely entrapped and inaccessible to the solvent. The molybdate is kept linked to the protein by hydrogen bonds to the oxygen atoms of the molybdate.

Molybdate transporters have been recently reported in more than 25 different bacterial species including *Rhodobacter capsulatus*, *Haemophilus influenzae* and the archaeon *Pyrococcus furiosus* [14–17]. Phylogenetic analyses of molybdate and sulphate-binding proteins have shown that ModA orthologs of *E. coli* and *A. vinelandii* belong to different sub-families, due to differences in the amino acid composition of the ligand-binding pocket, particularly the presence of the tyrosine residue at position 170, which, in the *E. coli* ortholog, forms hydrogen bonds with the molybdate anion [18]. Even bigger differences were noted for the anion-binding mode in *Afu* ModA [13]. The presence of a ModA ortholog in a plant pathogen was first reported following the sequencing of the complete genomes of *Xanthomonas axonopodis* pv. *citri* and *X. campestris* pv. *campestris* [19]. The successful expression and purification of a recombinant form of the *Xac* ModA was recently reported by our group [20]. The protein has a molecular weight of 25 kDa, binds molybdate and tungstate with high affinity and shows enhanced thermal stability following anion binding. Sequence alignment of the *Xac* ModA with different bacterial orthologs revealed a close similarity level with the *Eco* ModA. Moreover, crystals of the recombinant *Xac* ModA, obtained in the presence of molybdate, diffracted to a resolution of 1.7 Å [21]. In this work, we report the definition of the *Xac* ModA structure solved by molecular replacement based on the *Eco* ModA crystallographic structure.

2. Material and methods

2.1. Computational analysis

The nucleotide and corresponding amino acid sequences of the *X. citri modA* gene (gene ID: 1157429) were made available by the *Xanthomonas* genome project supported by Fundação de Amparo à Pesquisa do Estado de São Paulo (FAPESP) (http://genoma4.iq.usp.br/xanthomonas) (Genebank accession number AE011982). Search of ModA ortholog sequences were first carried out using the KEGG2 program of the Bioinformatics Center Institute for Chemical Research Kyoto University (www.genome.jp). The prediction of the signal peptide was made with the SignalP program (http://www.cbs.dtu.dk/services/SignalP/). The alignments of ModA amino acid sequences were carried out using the BLASTp and PsiBLAST, available at the National Center of Biotechnology Information server (http://www.ncbi.nlm.nih.gov/BLAST) and ClustalX [22]. Genedoc was used to edit the ClustalX results (http://www.psc.edu/biomed/genedoc/). The tree produced from the alignments was obtained using the Phylip tool (http://evolution.gs.washington.edu/phylip.html), and was visualized with Treeview (http://taxonomy.zoology.gla.ac.uk/rod/treeview.html).

2.2. Crystallization, data collection and processing

Xac ModA was expressed in *Eco* BL21(DE3) and purified in high amounts from the cytoplasm by immobilized metal affinity chromatography, as previously described [20]. Purified protein was submitted to crystallization trials at 18 °C using the sitting-drop vapour-diffusion technique. Crystallographic data from a single cryocooled crystal of ModA in the presence of sodium molybdate were collected at the protein crystallography beamline D03B-MX1 of the Brazilian Synchrotron Light Laboratory (LNLS) in Campinas, Brazil. The data set was processed using HKL2000 [23] and the CCP4 package (Collaborative Computational Project, Number 4, 1994). The crystal belongs to the $C222_1$ space group with unit cell dimensions $a=68.15$, $b=172.14$, $c=112.04$ Å and presents one trimer in the asymmetric unit [21]. Data processing statistics are shown in Table 1.

2.3. Structure solution, refinement and analysis

The structure of ModA bound to molybdate was solved by molecular replacement using the MOLREP program [24] and taking *Eco* ModA (PDB code 1AMF) as the search model. The resulting model was refined using REFMAC [25] and its stereochemistry validated with PROCHECK [26]. The program COOT [27] was used for model building. The final refinement statistics for the structure are listed in Table 1. The refined coordinates have been deposited in the PDB and received the entry code 2H5Y. Comparisons between *Xac* ModA and the orthologs were performed using the COOT program [27] and the Java Protein Dossier (JPD) of the Diamond Sting Suite (DMS 3.0) [28]. The cutoff distances used for the definition of hydrogen bonds, salt bridges, and aromatic interactions were 2.0–3.2 Å, 2.0–6.0 Å, and 4.0 Å, respectively. The secondary-structure matching (SSM) algorithm [29] implemented within the COOT program was used for the superposition of ModA structures and r.m.s.d. calculations. All pictures were generated with the PYMOL software [30].

3. Results and discussion

3.1. Overall structure of Xac ModA bound to molybdate

The structure of the molybdate-bound form of *Xac* ModA was obtained by molecular replacement using the *Eco* ModA coordinates as the searching template. The model was refined

Table 1
Data collection, processing and refinement statistics of the *Xac* ModA structure

Data collection	
Space group	$C222_1$
Unit cell parameters (Å)	$a=68.15$, $b=171.14$, $c=112.04$
Mosaicity (°)	0.5
Resolution limits (Å)	40.00–1.70 (1.76–1.70)
Mean I/σ(I) after merging	26.6 (3.3)
Completeness (%)	99.8 (99.3)
Multiplicity	5.7 (5.7)
R_{merge}	0.062 (0.415)
Number of reflections	417669
Number of unique reflections	72786 (7166)
Refinement	
R_{factor} [a]	0.168
R_{free} [a]	0.202
r.m.s.d. bond lengths (Å)	0.012
r.m.s.d. bond angles (°)	1.752
Total number of atoms/waters	6036/841
Average B factor (Å^2)	25.88
Ramachandran plot statistics by region (%) [b]	
Most favored	95.6
Allowed	4.4

Values in parenthesis correspond to data regarding the last resolution shell of 1.76–1.70 Å. Data collection was performed at 110 K with wavelength radiation of 1.421 Å and using a *MARCCD* detector to record the rotation data with $\Delta\varphi=1.0^{\circ}$.

[a] $R_{factor}=\Sigma||F_o(h)|-|F_c(h)||/\Sigma F_o(h)$, where $F_o(h)$ and $F_c(h)$ are observed and calculated amplitudes for reflection h. R_{free} is calculated by the same equation using 5% of the data, chosen randomly and omitted from the refinement.

[b] There were no residues in the generously allowed or disallowed regions of the plot.

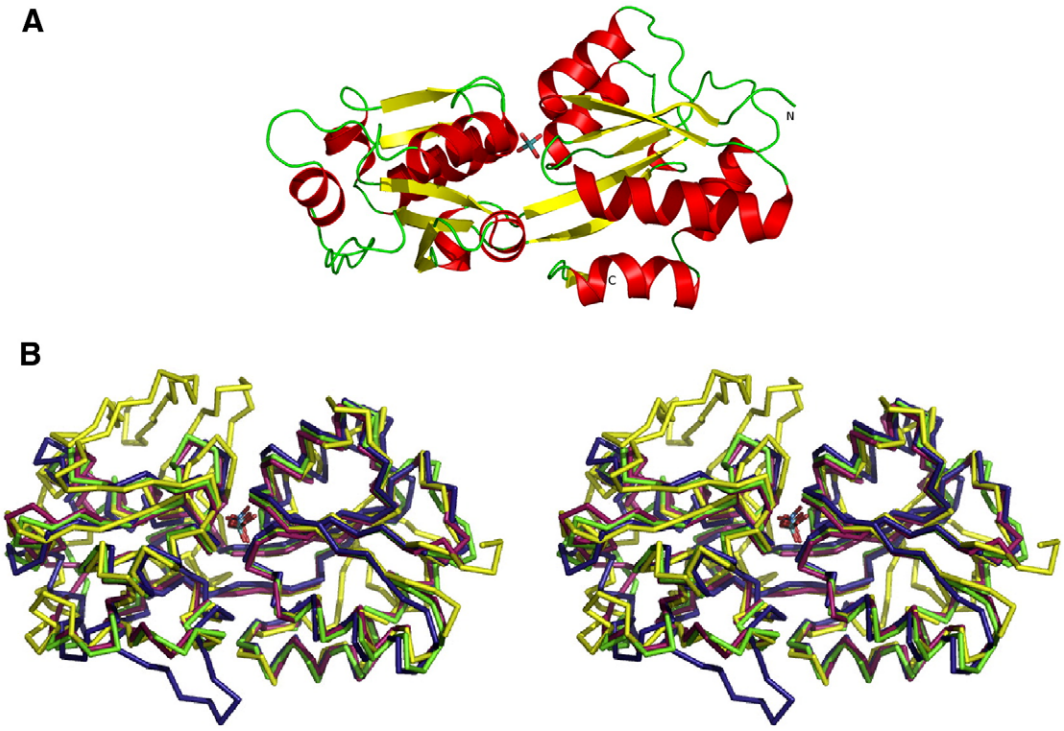

Fig. 1. *Xac* ModA structure and comparison with the orthologs. (A) Cartoon illustration of the *Xac* ModA tertiary structure with the molybdate ion shown in sticks at the binding site. The N-domain is on the right and the C-domain to the left of the molybdate anion. The N- and C-terminus are represented by the N and C letters, respectively. (B) ModA structures Cα-trace superposition: *Xac* (purple), *Eco* (green), *Avi* (blue) and *Afu* (yellow).

against data to a maximum resolution of 1.7 Å, yielding an R_{factor} of 0.168 and R_{free} of 0.202 (Table 1). The quality of *Xac* ModA model was validated with the PROCHECK program [26]. The Ramachandran plots revealed that 95.6% of the residues were in the most favored regions and no residue was placed in disallowed regions. The crystalline structure has three molecules of ModA in the asymmetric unit, all of which have a molybdate anion bound. Analysis of the monomer–monomer contacts within the unit cell using the PISA program [31] indicates that the trimer in the asymmetric unit and other complexation possibilities are formed due to crystallographic packing and should not be present in solution (data not shown). The r.m.s.d. between the individual monomers of the asymmetric unit is 0.3 Å. Similar to orthologs with solved three-dimensional structure, the *Xac* ModA has an ellipsoidal structure with dimensions of approximately 32 Å × 55 Å with a venus flytrap shape typical of ABC transporters' periplasmic protein. The protein is formed by two similar domains (α/β sandwich), named N- and C-domains, separated by the substrate-binding cleft (Fig. 1A). The N-domain is formed by residues 1–82 and 196–234, encompassing a region defined by one β-sheet with 5 strands surrounded by 5 α-helices, while the C-domain, spanning from residue 83 to 195, is formed by one 5-stranded β-sheet surrounded by 7 α-helices. As shown in Fig. 1B, the Cα alignment of the four ModA orthologs revealed that the similarity with the *Xac* ModA increases in the following order: *A. fulgidus*, *A. vinelandii* and *E. coli* with sequence identities of 22%, 26% and 52% and r.m.s.d. of 1.8 Å (214 residues aligned), 1.6 Å (211 residues aligned) and 1.1 Å (226 residues aligned) for C_α atoms, respectively. The higher r.m.s.d against the recently reported archaeal *Afu* ModA [13], reflects the presence of several structural differences including the presence of two big insertions that form an additional 4-stranded β-sheet (Fig. 1B). The *Xac* ModA presents inter domain connections characteristic of the group II hinge region of periplasmatic nutrient-binding proteins (amino acids 193–195 and amino acids 82–84) [32].

3.2. Ligand-binding pocket of Xac ModA

The molybdate-binding pocket mediates key protein–substrate interactions affecting both specificity and affinity of the bacterial ModA proteins. Among these interactions, the most important ones are seven hydrogen bonds between the protein and the molybdate anion oxygens (O1 to O4): $Ser_{12}/O^{\gamma}H-O4$, $Ser_{12}/NH-O4$, $Ser_{39}/NH-O2$, $Ser_{39}/O^{\gamma}H-O2$, $Ala_{125}/NH-O3$, $Val_{152}/NH-O1$ and $Tyr_{170}/O^{\eta}H-O3$ (Fig. 2). Four of these hydrogen bonds involve main chain amino groups located at the N-terminal region of α-helices, where the helical positive dipoles contribute for the stabilization of the molybdate negative charges (Fig. 2B). One exception concerning the helix dipole stabilization might be the Ser_{12} amino group interaction, located one residue prior to the helix and thus not aligned with the helix axial dipole. These electrostatic interactions are conserved between *Xac* and *Eco* ModA [12], but differ from *Avi* ModA in residues Ser_{12}, Ala_{125} and Tyr_{170}, which are changed to Asn, Tyr and Ala, respectively (Fig. 2C). The Ser_{12}Asn and

Ala_{125}Tyr changes do not affect the ligand hydrogen bonding pattern, but Tyr_{170}Ala prevents the $O^{\eta}H-O3$ hydrogen bond. This loss is compensated by the Ala_{11}Thr change in which the Thr residue forms a new $O^{\gamma}H-O1$ hydrogen bond found only in *Avi* ModA [11]. This network of hydrogen bonds is very specific for coordinating the tetrahedral disposition of the molybdate oxygens in bacteria. In contrast, the archaeal *Afu* ModA presents octahedral oxyanion coordination sustained by similar interactions and the additional ones provided by the changes Val_{123}Asp and Val_{152}Glu. These acid residues provide one side-chain's carboxylate oxygen each to form the octahedral geometry [13].

The selectivity for the anion has been explained by the size and polarity of the binding pocket [12,11]. Theoretical calculation using quantum mechanical/continuum dielectric methods have indicated that this selectivity is mainly due to the pocket size in the case of bacterial sulfate-binding proteins (SBP) [33], while with ModA, the most important effect would be anion desolvation [34]. Desolvating the larger molybdate anion is more energetically favored than the smaller sulfate. The polarity of the binding site affects the desolvation process by changing the environment dielectric constant. It has been shown that the ModA binding site has an apolar surface when compared

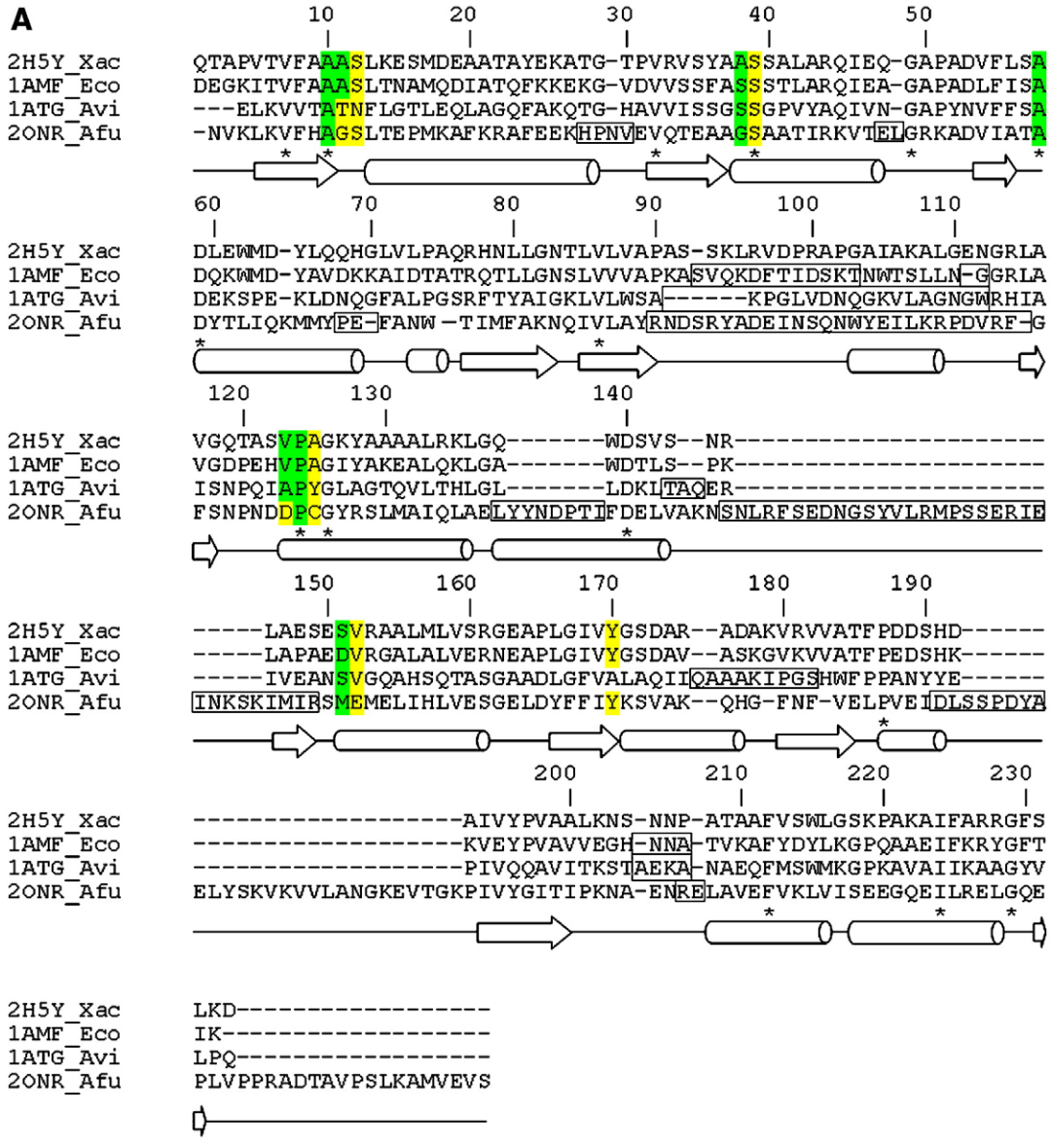

Fig. 2. The ModA binding site. (A) Amino acid structural alignment of the ModA orthologs from *Xac*, *Eco*, *Avi* and *Afu* produced with ClustalX [22] and corrected by visual inspection of the superposed structures. The numbering scheme follows the *Xac* ModA and the regions in boxes are structurally dissimilar from the *Xac* ModA structure. The asterisks underneath the sequences denote conservation, while the cylinders (helices) and arrows (β-strands) indicate the secondary structures present in *Xac* ModA. Amino acid residues involved in molybdate interactions are shown in yellow, when forming hydrogen bonds, or in green, when possessing carbon atoms within a 3.7 Å shell. (B) Ligand-binding pocket stereo view of *Xac* ModA evidencing the residues that interact with molybdate. Red cylinders indicate α-helices' axis and blue dashed lines indicate hydrogen bonds. The α-helix close to residue Ser_{12} is outside the limits of the figure. (C) Superposed ligand-binding site residues of ModA orthologs showing the equivalent residues in *Xac* (purple), *Eco* (green), *Avi* (blue) and *Afu* (yellow) proteins, respectively, that coordinate the ligand via hydrogen bonds. Residues in equivalent positions of the alignment that do not form hydrogen bonds are represented by small traces.

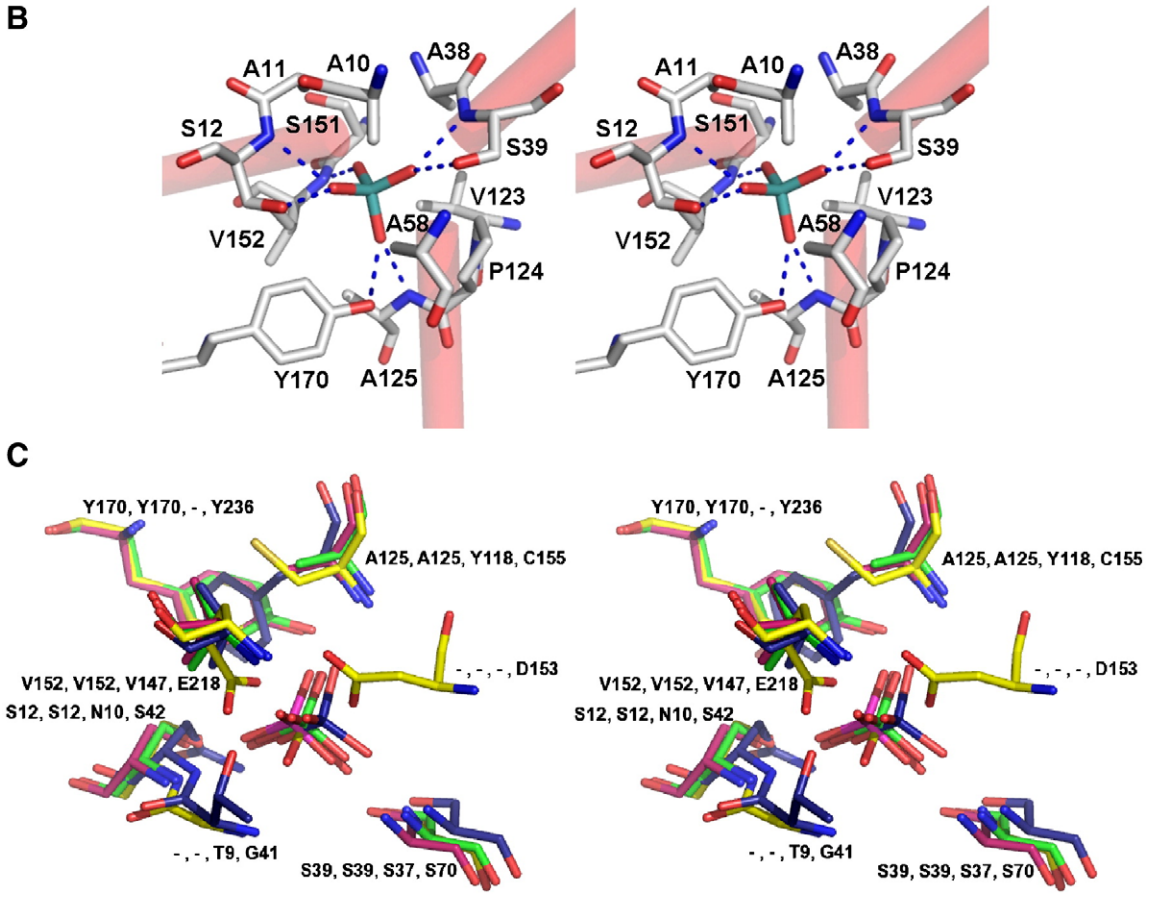

Fig. 2 (*continued*).

to the negative potential of the SBP cavity [11]. This difference arises from several residues that have carbon atoms in the binding pocket. In *Xac* ModA, residues Ala_{10}, Ala_{11}, Ala_{38}, Ala_{58}, Val_{123}, Pro_{124} and Ser_{151} have carbons located at less than 3.7 Å from the anion (marked in green in Fig. 2A). Residues Ala_{38} and Ser_{151} have not been previously cited as forming part of the binding pocket of bacterial ModAs, nevertheless they are certainly enhancing the molybdate selectivity by contributing to the formation of an apolar environment. In the case of these residues, the differences between *Xac* and *Eco* are: Ala_{38}–Ser and Ser_{151}–Asp; while the differences to the *Avi* structure are: Ala_{11}–Thr, Ala_{38}–Ser and Val_{123}–Ala. All these changes do not affect the positioning of the carbon atoms that form the binding pockets in the *Eco* or *Avi* orthologs. In the case of the *Afu* ModA, the carbon atoms forming the binding pocket are from residues occupying the same position in the structure (Fig. 2A), with the noticeable exception of the aspartate that replaces the Val_{123} and participates in the octahedral coordination.

The *Xac* ModA binds molybdate with a dissociation constant (K_d) of 0.29 μM [20]. Thus, molybdate affinity of *Xac* ModA is comparable to those reported for other bacterial molybdate-binding proteins such as the *Eco* K12 ModE (K_d=0.8 μM) [35], the *H. influenzae* Mop protein (K_d<1 μM) and the two *A. vinelandii* ModG binding sites (K_d of 10 nM and 10 μM) [5]. Two different K_d values for the molybdate-binding affinity of *Eco* ModA have been reported (20 nM and 3 μM), probably reflecting differences in the methodological approaches employed by the two research groups [36,37]. Since the amino acid residues directly interacting with molybdate were the same in *Xac* and *Eco* ModA, K_d differences may be reasoned by other residues indirectly affecting the attraction, binding and release of the anion to the oxyanion-binding pockets of the two proteins.

3.3. Sequence homology and phylogenetic analysis

The *Xac modA* gene encodes a 257 residue protein, including a putative 24 amino acid-long signal peptide. Amino acid sequence alignment of *Xac* ModA and twelve bacterial and one archaeal ModA orthologs revealed two highly conserved regions including all residues directly interacting with molybdate. An unrooted phylogenetic tree generated from the amino acid sequence of bacterial ModA and the recently reported sequence of the archaeal *Afu* ModA protein [13], revealed the presence of three main branches or families (Fig. 3). The first branch (Family 1) included the ModA orthologs expressed by enterobacteria including *E. coli*, *Salmonella typhimurium*, *Shigella flexneri* and *Yersinia pestis*. The second group (Family 2) encompassed ModA orthologs found in the genomes of plant-interacting bacterial species, such as the *X. citri*, *X. campestris*, *Mezorhizobium loti*, *Sinorhizobium meliloti* and *Agrobacterium tumefaciens* orthologs. Finally, the last and third phylogenetic group (Family 3) was characterized by a group of the more distantly related species

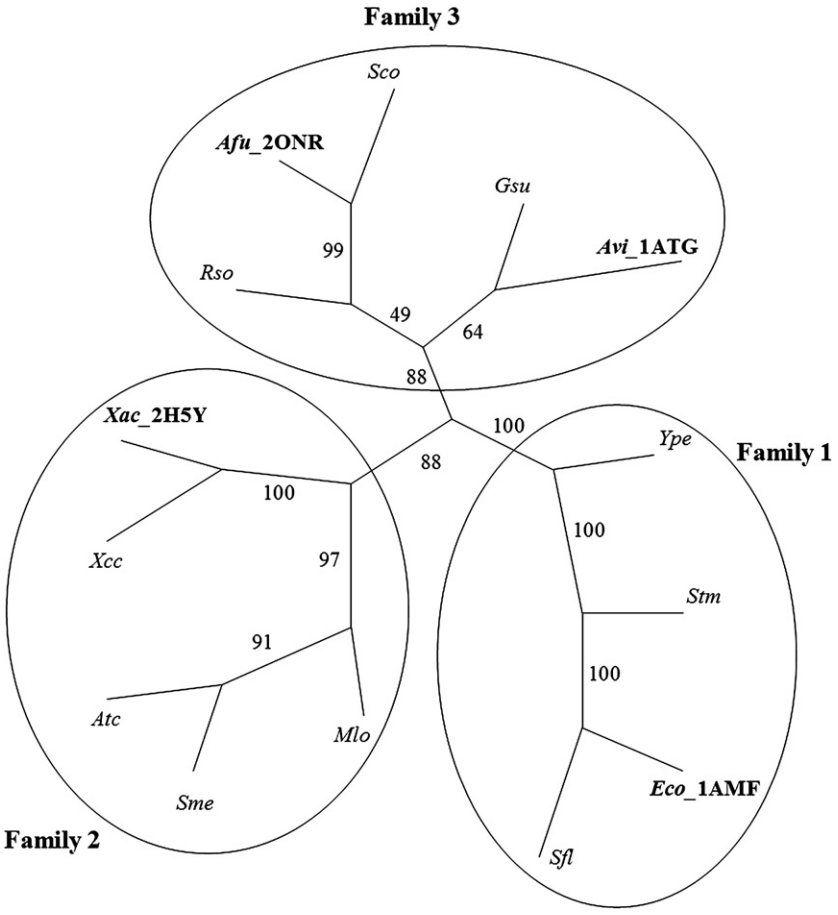

Fig. 3. Phylogenetic analysis of *Xac* ModA and orthologs. Unrooted tree generated with PHYLIP program by maximum parsimony with bootstrap of 100. The *Xac* (PDB code 2H5Y), *Eco* (PDB code 1AMF), *Avi* (PDB code 1ATG) and *Afu* (PDB code 2ONR) ModAs are marked in bold.

including soil bacteria such as *A. vinelandii, Geobacter sulfurreducens*, *Streptomyces coelicolor*, *Ralstonia solanacearum* and the archaeon *A. fulgidus*. Analysis of each group showed that enterobacteria and plant-interacting bacteria share high sequence identity values ranging from 44% to 91% (data not shown). Differently, the sequence comparison for soil bacteria ModA excluding the sequence from *Afu* ModA, showed a larger diversity as demonstrated by the low sequence identity values (maximum of 15%). Phylogenetic analysis of the ModA orthologs including the four proteins with solved structure showed that the oxyanion-binding pocket residues are not solely responsible for differences in the phylogenetic classification such as was suggested before [11,18]. Fig. 3 reveals that *Eco* and *Xac* ModA belong to different families in spite of the conserved residues involved in the hydrogen bond network of the oxyanion-binding pockets. On the other hand, *Avi* and *Afu* ModA proteins were classified in the same sequence similarity family despite the differences in their binding pocket amino acid residues.

The recent description of the complete structure of the molybdate transporter of *A. fulgidus* [13] together with the present elucidation of the *Xac* ModA structure, will certainly contribute for the understanding of the molybdate transport in *X. citri*, including the definition of ModA amino acid residues interacting with the membrane-bound ModB component.

Acknowledgments

This work was supported by Fundação de Amparo à Pesquisa do Estado de São Paulo (FAPESP, SMolBNet grants 01/07540-3 and 00/10266-8), Conselho Nacional de Desenvolvimento Científico e Tecnológico (CNPq) and Associação Brasileira de Tecnologia de Luz Síncrotron (ABTLuS). C.S.-P. also thanks the Academy of Sciences for the Developing World (TWAS) for the fellowship. We also thankfully acknowledge the support from Dr. Rogério Meneghini.

References

[1] R. Hille, Molybdenum and tungsten in biology, Trends Biochem. Sci. 27 (2002) 360–367.
[2] R.N. Pau, D.M. Lawson, Transport, homeostasis, regulation, and binding of molybdate and tungstate to proteins, Met. Ions Biol. Syst. 39 (2002) 31–74.
[3] K.V. Rajagopalan, J.L. Johnson, The pterin molybdenum cofactors, J. Biol. Chem. 267 (1992) 10199–10202.
[4] R.N. Pau, W. Klipp, S. Leimkuhler, Molybdenium transport, processing and gene regulation. Iron and related transition metals in microbial metabolism, in: G. Winkelmann, C.J. Carrano, N.J. Newark (Eds.), Transition Metals in Microbial Metabolism, Harwood Academic Publishers, 1997, p. 217–234.
[5] A.K. Duhme, W. Meyer-Klaucke, D.J. White, L. Delarbre, L.A. Mitchenall, R.N. Pau, Extended X-ray absorption fine structure studies on periplasmic and intracellular molybdenum-binding proteins, J. Biol. Inorg. Chem. 4 (1999) 588–592.

[6] A.M. Grunden, W.T. Self, M. Villain, J.E. Blalock, K.T. Shanmugan, An analysis of the binding of repressor protein ModE to modABCD (Molybdate Transport) operator/promoter DNA of *Escherichia coli*, J. Biol. Chem. 274 (1999) 24308–24315.
[7] D.G. Gourley, A.W. Schuttelkopf, L.A. Anderson, N.C. Price, D.H. Boxer, W.N. Hunter, Oxyanion binding alters conformation and quaternary structure of the C-terminal domain of the transcriptional regulator mode. Implications for molybdate-dependent regulation, signaling, storage, and transport, J. Biol. Chem. 276 (2001) 20641–20647.
[8] L. Delarbre, C.E. Stevenson, D.J. White, L.A. Mitchenall, R.N. Pau, D.M. Lawson, Two crystal structures of the cytoplasmic molybdate-binding protein ModG suggest a novel cooperative binding mechanism and provide insights into ligand-binding specificity, J. Mol. Biol. 18 (2001) 1063–1079.
[9] R. Tam, M.H. Saier Jr, Structural, functional, and evolutionary relationships among extracellular solute-binding receptors of bacteria, Microbiol. Rev. 57 (1993) 320–346.
[10] A.M. Grunden, K.T. Shanmugam, Molybdate transport and regulation in bacteria, Arch. Microbiol. 168 (1997) 345–354.
[11] D.M. Lawson, C.E. Williams, L.A. Mitchenall, R.N. Pau, Ligand-size is the major determinant of specificity in periplasmic oxyanion-binding proteins: the 1.2 Å resolution crystal structure of *Azotobacter vinelandii* ModA, Structure 6 (1998) 1529–1539.
[12] Y. Hu, S. Rech, R.P. Gunsalus, D.C. Rees, Crystal structure of molybdate-binding protein ModA, Nat. Struct. Biol. 4 (1997) 703–707.
[13] K. Hollenstein, D.C. Frei, K.P. Locher, Structure of an ABC transporter in complex with its binding protein, Nature 446 (2007) 213–215.
[14] S. Rech, U. Deppenmeier, R.P. Gunsalus, Regulation of the molybdate transport operon, modABCD, of *Escherichia coli* in response to molybdate availability, J. Bacteriol. 177 (1995) 1023–1029.
[15] F. Luque, L.A. Mitchenall, M. Chapman, R. Cristine, R.N. Pau, Characterization of genes involved in molybdenium transport in *Azotobacter vinelandii*, Mol. Microbiol. 7 (1993) 457–459.
[16] R.D. Fleischmann, M. Adams, O. White, R.A. Clayton, E.F. Kirkness, et al., Whole-genome random sequencing and assembly of *Haemophilus influenzae* Rd, Science 269 (1995) 496–512.
[17] L.E. Bevers, P.L. Hagedoorn, G.C. Krijger, W.R. Hagen, P.L. Hagedoorn, Tungsten transport protein A (WtpA) in *Pyrococcus furiosus*: the first member of a new class of tungstate and molybdate transporters, J. Bacteriol. 188 (2006) 6498–505.
[18] W.T. Self, A.M. Grunden, A. Hasona, K.T. Shanmugam, Molybdate transport, Res. Microbiol. 152 (2001) 311–321.
[19] A.C. da Silva, J.A. Ferro, F.C. Reinach, C.S. Farah, et al., Comparison of the genomes of two *Xanthomonas* pathogens with differing host specificities, Nature 23 (2002) 459–463.
[20] A. Balan, C.P. Santacruz, A. Moutran, R.C. Ferreira, C.H.I. Ramos, J. Medrano, L.C. Ferreira, The Molybdate-binding protein (ModA) of the phytopathogen *Xanthomonas axonopodis* pv. *Citri*, Protein Exp. Purif. 50 (2006) 215–222.
[21] C.P. Santacruz, A. Balan, L.C. Ferreira, J.A.R. Barbosa, Crystallization, data collection and phasing of molybdate-binding protein of the phytopathogen *Xanthomonas axonopodis* pv *citri*, Acta Crystallograph. Sect. F Struct. Biol. Cryst. Commun. 62 (2006) 289–291.
[22] J.D. Thompson, T.J. Gibson, F. Plewniak, F. Jeanmougin, D.G. Higgins, The ClustalX windows interface: flexible strategies for multiple sequence alignment aided by quality analysis tools, Nucleic Acids Res. 25 (1997) 4876–4882.
[23] Z. Otwinowski, W. Minor, Processing of X-ray diffraction data collected in oscillation mode, Methods Enzymol. — Macromol. Crystallogr. 276 (1997) 307–326.
[24] A. Vagin, A. Teplyakov, An approach to multi-copy search in molecular replacement, Acta Crystallogr., D Biol. Crystallogr. 56 (2002) 1622–4.
[25] G.N. Murshudov, A.A. Vagin, E.J. Dodson, Refinement of macromolecular structures by the maximum-likelihood method, Acta Crystallogr. D53 (1997) 240–255.
[26] R.A. Laskowski, M.W. MacArthur, D.S. Moss, J.M. Thornton, PROCHECK: a program to check the stereochemical quality of protein structures, J. Appl. Cryst. 26 (1993) 283–291.
[27] P. Emsley, K. Cowtan, Coot: model-building tools for molecular graphics, Acta Crystallogr., D Biol. Crystallogr 60 (2002) 2126–2132.
[28] G. Neshich, L.C. Borro, R.H. Higa, P.R. Kuser, M.E. Yamagishi, E.H. Franco, J.N. Krauchenko, et al., The Diamond STING server, Nucleic Acids Res. 33 (2005) 29–35.
[29] E. Krissinel, K. Henrick, Secondary-structure matching (SSM), a new tool for fast protein structure alignment in three dimensions, Acta Crystallogr., D Biol. Crystallogr. 60 (2004) 2256–2268.
[30] W.L. Delano, The PyMOL molecular graphics system on world wide web, http://www.pymol.org, 2002.
[31] E. Krissinel, K. Henrick, Inference of macromolecular assemblies from crystalline state, J. Mol. Biol. 372 (2007) 774–797.
[32] F.A. Quiocho, P.S. Ledvina, Atomic structure and specificity of bacterial periplasmic receptors for active transport and chemotaxis: variation of common themes, Mol. Microbiol. 20 (1996) 17–25.
[33] J.W. Pflugrath, F.A. Quiocho, Sulphate sequestered in the sulphate-binding protein of *Salmonella typhimurium* is bound solely by hydrogen bonds, Nature 314 (1985) 257–260.
[34] T. Dudev, C. Lim, Oxyanion selectivity in sulfate and molybdate transport proteins: an *ab initio*/CDM study, J. Am. Chem. Soc. 126 (2004) 10296–10305.
[35] L.A. Anderson, T. Palmer, N.C. Price, S. Bornemann, D.H. Boxer, R.N. Pau, Characterisation of the molybdenum-responsive ModE regulatory protein and its binding to the promoter region of the modABCD (molybdenum transport) operon of *Escherichia coli*, Eur. J. Biochem. 246 (1997) 119–126.
[36] J. Imperial, M. Hadi, N.K. Amy, Molybdate binding by ModA, the periplasmic component of the *Escherichia coli* mod molybdate transport system, Biochem. Biophys. Acta 1370 (1998) 337–346.
[37] S. Rech, C. Wolin, R.P. Gunsalus, Properties of the periplasmic ModA molybdate-binding protein of *Escherichia coli*, J. Biol. Chem. 271 (1997) 2557–2562.